*Materials Transactions*, Vol. 49, No. 1 (2008) pp. 24 to 30
Special Issue on Severe Plastic Deformation for Production of Ultrafine Structures and Unusual Mechanical Properties: Investigating Role of High-Density Lattice Defects


# Grain Boundary Structure of Ultrafine Grained Pure Copper Fabricated by Accumulative Roll Bonding

Ken-ichi Ikeda[1], Kousuke Yamada[2,*1], Naoki Takata[3], Fuyuki Yoshida[1,*2], Hideharu Nakashima[1] and Nobuhiro Tsuji[3]

[1]*Department of Electrical and Materials Science, Faculty of Engineering Sciences, Kyushu University, Kasuga 816-8580, Japan*
[2]*Department of Molecular and Material Sciences, Interdisciplinary Graduate School of Engineering Sciences, Kyushu University, Kasuga 816-8580, Japan*
[3]*Department of Adaptive Machine Systems, Graduate School of Engineering, Osaka University, Suita 567-0871, Japan*

Grain boundary structures of ultrafine grained pure copper (Cu) fabricated by the accumulative roll bonding (ARB) have been studied. The atomic structures of grain boundaries in the ARB processed Cu (ARB-Cu) were observed by high resolution electron microscopy. In order to compare the grain boundaries in the ARB-Cu with equilibrium grain boundaries, the grain boundary energy and structure of symmetric tilt boundaries with ⟨110⟩ common axis in pure Cu were computed by molecular dynamics simulation (MD). The low angle boundaries in the ARB-Cu were basically described by conventional dislocation model and simultaneously there were some local structures having certainly high energy configurations. The grain boundaries with large misorientation in the ARB-Cu are basically described by the structural units predicted for the normal grain boundaries by MD. The present results indicate that the atomic structures of the boundaries in the Cu severely deformed by the ARB are rather similar to those of the equilibrium grain boundaries, except for the local distortions. [doi:10.2320/matertrans.ME200715]

(Received July 5, 2007; Accepted August 22, 2007; Published October 3, 2007)

***Keywords:*** *copper, accumulative roll bonding, grain boundary structure, structural unit model, high resolution electron microscopy*

## 1. Introduction

Severe plastic deformation (SPD) of metallic materials above equivalent strain of 4–5 can produce ultrafine grained (UFG) microstructures where the mean grain size is much smaller than 1 μm. The UFG materials fabricated by SPD perform excellent mechanical properties like quite high strength and good superplasticity.[1)] Generally speaking, properties of polycrystalline materials are strongly affected by atomic structure of their grain boundaries.[2–6)] Therefore, it is expected that the mechanical properties of the UFG materials having numerous number of grain boundaries are governed by the atomic structure of the grain boundaries. Valiev *et al.*[1)] have actually insisted that the "non-equilibrium grain boundary", that is composed of high energy defects like disclinations and grain boundary dislocations, determines the unique properties of the UFG materials fabricated by SPD. However, the atomic structure of the grain boundaries in the SPD/UFG materials has been rarely studied except for the study by Horita *et al.*[7)] Thus, the nature of non-equilibrium grain boundaries and their effects on properties of the SPD/UFG materials are still unclear.

On the other hand, the atomic structure of normal "equilibrium" grain boundaries has been fairly studied by theoretical and experimental approaches. Sutton and Vitek[8)] investigated the atomic structure of symmetric tilt boundaries in face-centered cubic (f.c.c.) metals and proposed the structural unit model that can estimate the grain boundary energy and structure. Morita and Nakashima[9)] showed that the atomic structure of the symmetric tilt boundaries with ⟨001⟩ common axis (⟨001⟩ symmetric tilt grain boundaries; ⟨001⟩ STGBs) observed in molybdenum, which was prepared by floating-zone technique, coincided well with their predicted structure that can be described by the structural unit model. In other metals, the theoretical studies on the relation between the energy and atomic structure of various STGBs also indicated the validity of the structural unit model.[10–12)]

In this study, the atomic structure of the grain boundaries in the UFG Cu fabricated by the accumulative roll bonding (ARB) process, which is a kind of SPD process,[13)] was observed by high resolution transmission electron microscopy (HRTEM). Furthermore, in order to compare the grain boundaries in the ARB-Cu with equilibrium grain boundaries, the grain boundary energy and structure of ⟨110⟩ STGBs in pure Cu were computed by molecular dynamics (MD) simulation. The electron back-scattering diffraction (EBSD) measurement in the previous study[14)] has found that the ARB-Cu had a texture composed of ⟨110⟩ // TD (the transverse direction of the sheet), so that the present observation of the grain boundary structure by HRTEM was carried out along TD. The grain boundary energy and structure simulation was also done for ⟨110⟩ STGBs. From these results, an atomic structure of the grain boundaries in the SPD processed materials was discussed.

## 2. Experimental

Oxygen-free 99.99% purity copper sheet was used in this study. The Cu sheets were heavily deformed by ARB. Figure 1 shows the principle of the ARB process.[13)] The starting sheet was 1 mm thick, 20 mm wide and 335 mm long. After degreasing and wire-brushing the contact surfaces, two pieces of the sheets were stacked and then roll-bonded by 50% reduction in thickness by one pass without lubricant at

*1Graduate Student, Kyushu University, Present address: Fuji Heavy Industries, Ltd.
*2Present address: Nakayama Steel Works, Ltd., Osaka 511-8551, Japan

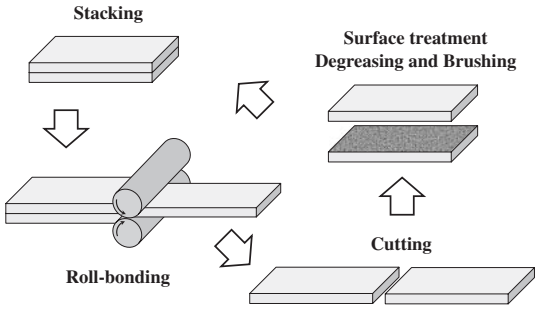


Fig. 1 Production process of the ARB processed material.

room temperature. The roll-bonded sheet was cut into two, and then the same procedure was repeated up to six cycles. Therefore, the specimens deformed to total equivalent strain from 1.6 to 4.8 were obtained.

Samples deformed by two or six cycles ARB (2cARB-Cu or 6cARB-Cu, hereafter) were examined by HRTEM. For HRTEM observation, thin foils perpendicular to TD of the ARB processed sheets were prepared by mechanical polishing and twin-jet electro-polishing. The electro-polishing was conducted using a 30 vol% phosphoric acid aqua solution at 293 K and about 45 mV. HRTEM observation was carried out in JEOL JEM-2000EX/T equipped with a top entry goniometer stage operated at 200 kV.

For MD simulation, 24 different ⟨110⟩ STGBs in Cu were prepared. The misorientation angle of ⟨110⟩ STGB indicates the angle between {110} planes involving the common ⟨110⟩ axis in the adjacent crystals. The principle and the geometric approach of the preparing the unit cell of bicrystal for the MD simulation have been reported previously.[12,15] In this study, the MD simulation was carried out using WinMASPHYC Pro 2.0 program developed by Fujitsu, Ltd. The Long Range Finnis Sinclair (LRFS) potential[16] was used as the interatomic potential function. The NTP ensemble (the number of atoms, temperature and pressure constant simulation) was used in this study under the conditions of 0 K and 0.1 MPa. The grain boundary energy ($\gamma_{gb}$) was estimated by the following equation,

$$\gamma_{gb} = \frac{U_{gb} - U_B}{2S}, \tag{1}$$

where $U_{gb}$ and $U_B$ represent the internal energy of the simulated cells with grain boundaries and that of the cells of a perfect crystal, respectively. $S$ represents the area of grain boundaries. Several initial atomic structures were prepared for the grain boundaries with the same misorientation angles. The internal energy of all the atomic structures was estimated by MD simulation, and then the lowest energy among the energies of all the initial structures was determined as $U_{gb}$. The corresponding atomic structure was adopted as the most stable structure for the grain boundary with the specific orientation relationship (equilibrium grain boundary).

## 3. Results and Discussion

### 3.1 The grain boundary energy and structure of ⟨110⟩ STGB simulated by MD

Figure 2 shows the grain boundary energy of most stable ⟨110⟩ STGBs in Cu with various misorientations evaluated by the MD simulation, which correspond to so-called "equilibrium" STGBs. This figure clearly shows that the grain boundary energy strongly depends on the misorientation angle. Two deep energy cusps were found at 70.5° and 129.5° which correspond with the {111} $\Sigma$3 and {113} $\Sigma$11 orientation relationship. This misorientation angle dependence for Cu is good agreement with the calculated result[17] and the experimental result.[18] Figure 2 also shows atomic structures of the ⟨110⟩ STGBs with certain misorientations. Here, the open circles and the filled circles represent the atoms on two adjacent {220} planes perpendicular to the paper, and the position of circles with a dot represents the coincidence site lattice (CSL) point sharing two adjacent {220} planes on the boundary. By connecting the nearest-neighbor atoms, specific atomic arrangements form along the boundary plane. This atomic arrangement is called the structural unit. It was found that {331} $\Sigma$19, {111} $\Sigma$3 or {113} $\Sigma$11 STGBs consisted of single structural unit. {110} $\Sigma$1 and {001} $\Sigma$1 are single crystals, so that these structures also have the single structural unit. Systematically organizing the atomic structures of ⟨110⟩ STGBs in term of the structural unit model led to the unique hierarchy showing that the atomic structures of ⟨110⟩ STGBs with any misorientations could be described by the combination of five different structural units ({110} $\Sigma$1, {331} $\Sigma$19, {111} $\Sigma$3, {113} $\Sigma$11 and {001} $\Sigma$1). For example, {221} $\Sigma$9 STGB, of which misorientation angle is between the angles of {331} $\Sigma$19 and {111} $\Sigma$3 STGBs, are composed of {331} $\Sigma$19 and {111} $\Sigma$3 structural units, as shown in Fig. 2. The correlation between atomic structure and energy has been discussed in the previous article.[15] It can be concluded that the atomic structure of all "equilibrium" ⟨110⟩ STGBs in Cu can be characterized by the concept of structural unit model.

### 3.2 Ultrafine grained microstructure

Figure 3 shows TEM microstructures of pure Cu ARB processed by (a) 2 cycles and (b) 6 cycles. The TEM observation revealed that a large amount of grain boundaries along ND could be observed within the elongated microstructures of both the 2cARB-Cu and 6cARB-Cu. While the 2cARB-Cu showed microstructure involving dense dislocation substructures corresponding to tangled dislocations and dislocation cells, the dislocation density seems rather decreased in the finely subdivided "lamellar boundary structure" of the 6cARB-Cu. The previous work has revealed that the 6cARB-Cu showed UFG microstructure with mean lamellar spacing of about 0.2 μm.[14] These observed microstructures were similar to one which has been reported in the heavily rolled materials.[19] Therefore, the grain boundaries within microstructures of the ARB processed Cu observed in this study can be considered characterized by the lamellar boundary and the interconnecting boundary.[20]

### 3.3 Low angle boundary

Figure 4 shows the TEM images of the low angle boundaries in 6cARB-Cu. In order to evaluate the misorientation angles, TEM/Kikuchi line method and diffraction pattern method were used. The Kikuchi patterns and

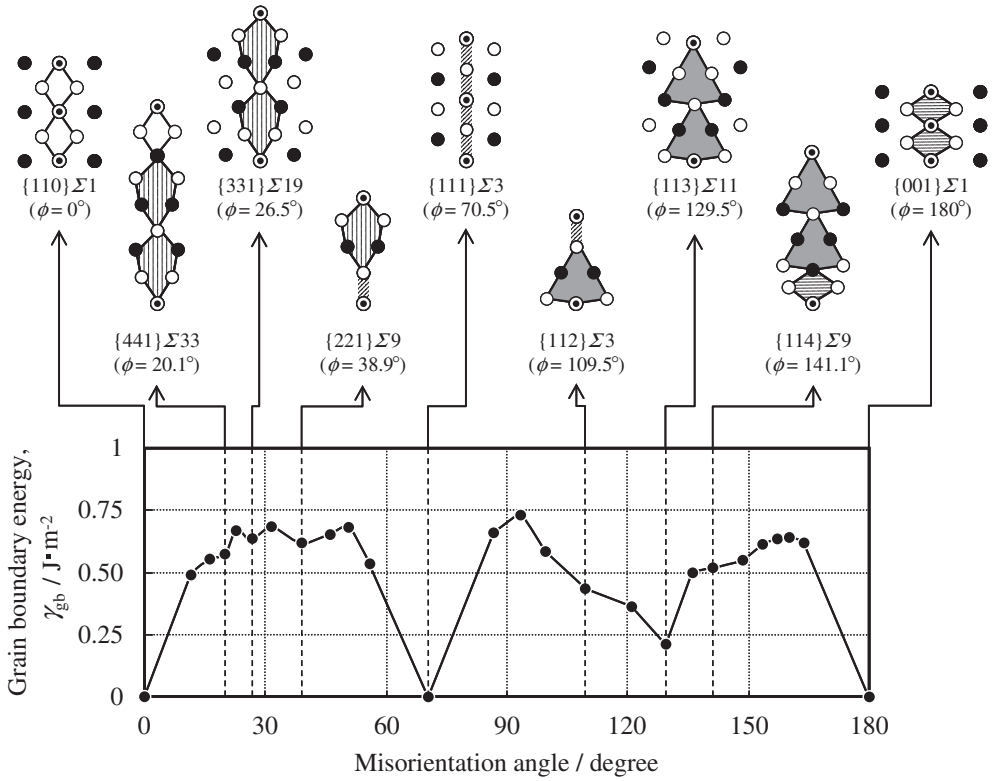


Fig. 2 The grain boundary energy and the atomic structure of equilibrium ⟨110⟩ STGBs of copper obtained by MD simulation.

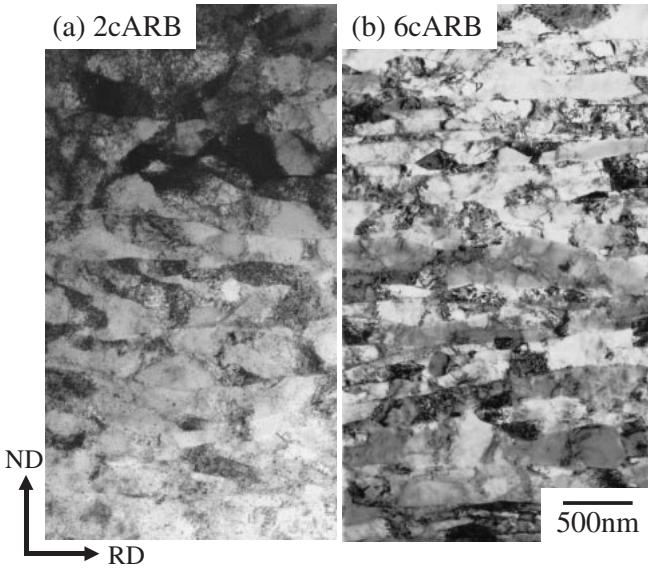


Fig. 3 TEM images of microstructure in pure copper ARB processed by (a) 2 cycles and (b) 6 cycles. The microstructures were observed from TD.

diffraction pattern are superimposed in Fig. 4. Analyzing these patterns revealed that the misorientation angles of the low angle boundaries were (a) 11° and (b) 14°, respectively. Figure 5 shows the HRTEM images of the low angle boundaries in the square regions in Figs. 4(a) and 4(b), respectively. Figure 5(a) shows that the 11° low angle boundary has the periodic edge dislocation arrangement. Their spacing was about 1.25 nm. According to the dislocation model for low angle boundaries,[21] the edge dislocation spacing in a low angle boundary, $D$, should be given by

$$D = \frac{b}{2\sin(\theta/2)}, \tag{2}$$

where $b$ is the magnitude of Burgers vector and $\theta$ is the misorientation angle. When $b = (a/2)\langle 110\rangle$ ($= 0.256$ nm) in Cu, $D$ should be 1.34 nm for the 11° low angle boundary from eq. (2), which is close to the value (1.25 nm) obtained from Fig. 5(a). Figure 5(b) shows the HRTEM image of the 14° low angle boundary in 6cARB-Cu. In the upper side of this image, the edge dislocations again existed periodically and their spacing was about 1.05 nm. The equation (2) gives $D = 1.05$ nm for the 14° low angle boundary, which again coincides with the experimental result (1.05 nm). From these results, it can be concluded that both boundaries are well described by the conventional dislocation model. However, the grain boundary planes were not straight but curved in short distances, so that the dislocations arrays were not straight as well. Furthermore, lattice bending and many dislocations gathering nearby a part of the boundary were observed, as shown in the square region in Fig. 5(b). Horita *et al.*[7] reported similar curved boundary planes and dense dislocation region near the grain boundary in the Al-Mg solid solution severely deformed by high pressure torsion (HPT). They called it a kind of non-equilibrium boundary. It should be emphasized again that the present low angle boundaries in the ARB-Cu was basically described by conventional dislocation model and simultaneously there were some local distorted structures having certainly high energy configurations.

### 3.4 Twin boundary

According to previous studies,[22–24] deformation twinning

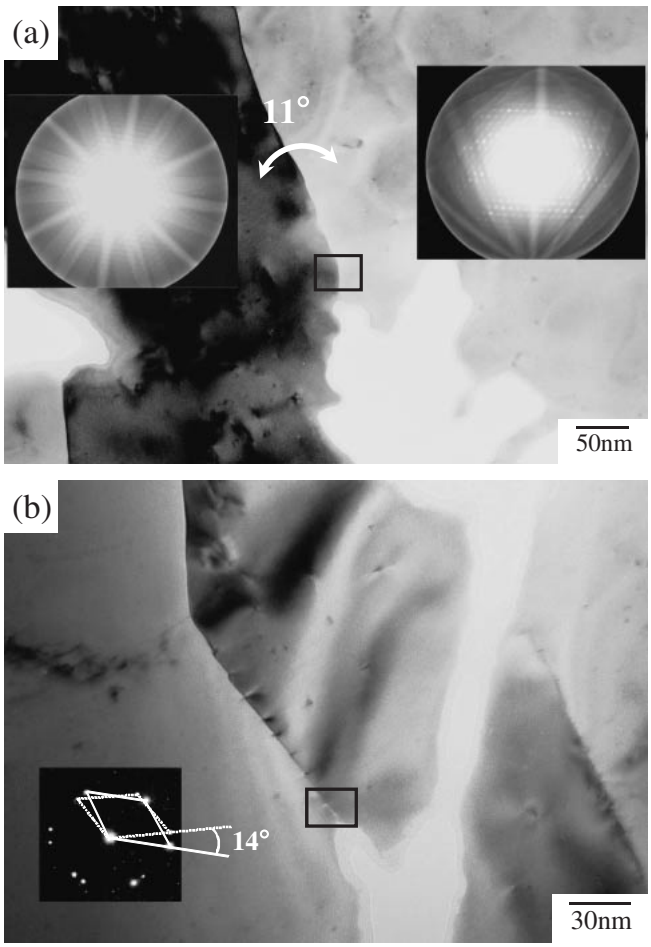


Fig. 4 TEM images and Kikuchi line patterns and diffraction pattern of low angle boundaries in 6cARB-Cu. (a) 11° low angle boundary, (b) 14° low angle boundary.

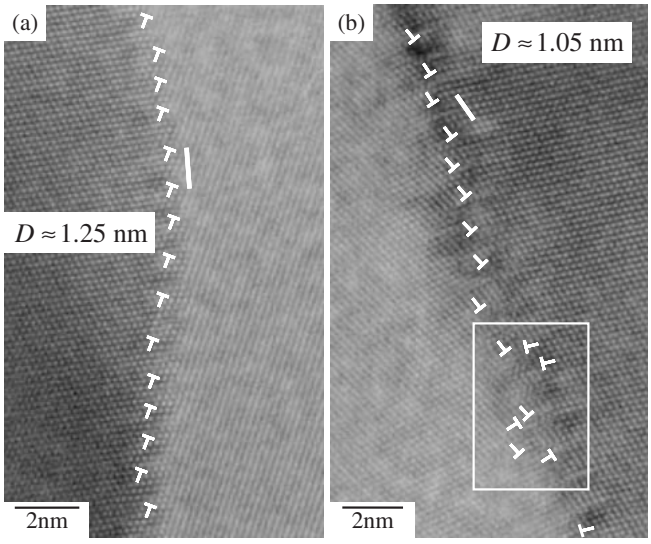


Fig. 5 HRTEM images of low angle boundaries in 6cARB-Cu. (a) 11° low angle boundary, (b) 14° low angle boundary.

is unusual in Cu except for the deformation at very low temperature or at very high speed. Zhao *et al.*[22] reported that the ductility and strength of pure Cu bar processed by equal channel angular pressing at ambient temperature (ECAP-Cu), cryogenic drawing and rolling at 77 K (ECAP+D+R-Cu) were simultaneously improved than those of ECAP-Cu. In their paper, it was also found that ECAP+D+R-Cu had many nano-twins with wavy boundary plane lead to a high strength. Furthermore, it was reported that 99.98% purity Cu deformed by torsion under pressure at ambient temperature had no twins.[23]

However, it is noteworthy that very fine twins in nanometer dimensions were observed in the present Cu specimens ARB processed at ambient temperature. Figures 6(a) and (b) show the nano-twins observed in 2cARB-Cu and 6cARB-Cu, respectively. The width of twins is about 6–8 nm. Figures 6(c) and (d) show the HRTEM images of the twins in the square regions of Figs. 6(a) and (c), respectively. These twins are very thin and consist of just about 30 atomic layers of {111} planes. Therefore, it can be considered that these twins are deformation twins. The twin boundaries are quite straight and there are no distortions in atomic configurations. From these HRTEM images, the atomic structure of the twin boundaries in the ARB-Cu is the same as that of annealing twins in recrystallized Cu and agrees with that of simulated {111} $\Sigma 3$ STGB as well. From these results, it is concluded that the deformation twins could be observed in the ARB-Cu and the twin boundary structure was the same as the normal $\Sigma 3$ twin boundary.

### 3.5 High angle boundary

Figure 7 shows TEM image and HRTEM image of high angle tilt boundaries of the 2cARB-Cu. In Fig. 7(a), the macroscopic TEM observation revealed that the grain boundary sat on a certain plane being near-parallel to RD. This implies that the observed grain boundary corresponds to lamellar boundary within the elongated microstructure. Figure 7(b) shows the HRTEM image of high angle boundary in the square region of Fig. 7(a). The FFT (Fast Fourier Transform) image of the dotted square region in the HRTEM images is shown in Fig. 7(c). The FFT analysis revealed that the observed high angle boundaries in the 2cARB-Cu had a misorientation of 29°, which was close to ⟨110⟩ $\Sigma 19$ orientation relationship (common axis: ⟨110⟩, rotation angle: 26.5°). The stable atomic structure of the {331} $\Sigma 19$ STGB obtained by MD simulation is shown in Fig. 7(d). Comparing with the atomic structure calculated by MD simulation, the observed grain boundary is an asymmetric tilt boundary (ATGB) having near $\Sigma 19$ orientation relationship. From Figs. 7(b) and (c), it was found that this boundary plane of right crystal was composed of facets parallel to {111} close-packed plane. Figure 7(c) also shows that the major part of grain boundary structure is composed of the structural units similar to that for the {331} $\Sigma 19$ grain boundary. The observed atomic configuration shows somewhat irregular-shape structural unit comparing with the kite-shaped structural unit evaluated by MD simulation. It should be noted that the boundaries simulated in the present study are all "symmetric" tilt boundaries (STGB) but the boundary in Fig. 7 is "asymmetric" one (ATGB). The atomic structure of ATGB in the artificial molybdenum bicrystal (body centered cubic structure) was previously reported.[25] The paper concluded that the grain boundary structure of ATGB in molybdenum can be described as a mixture of two kinds of

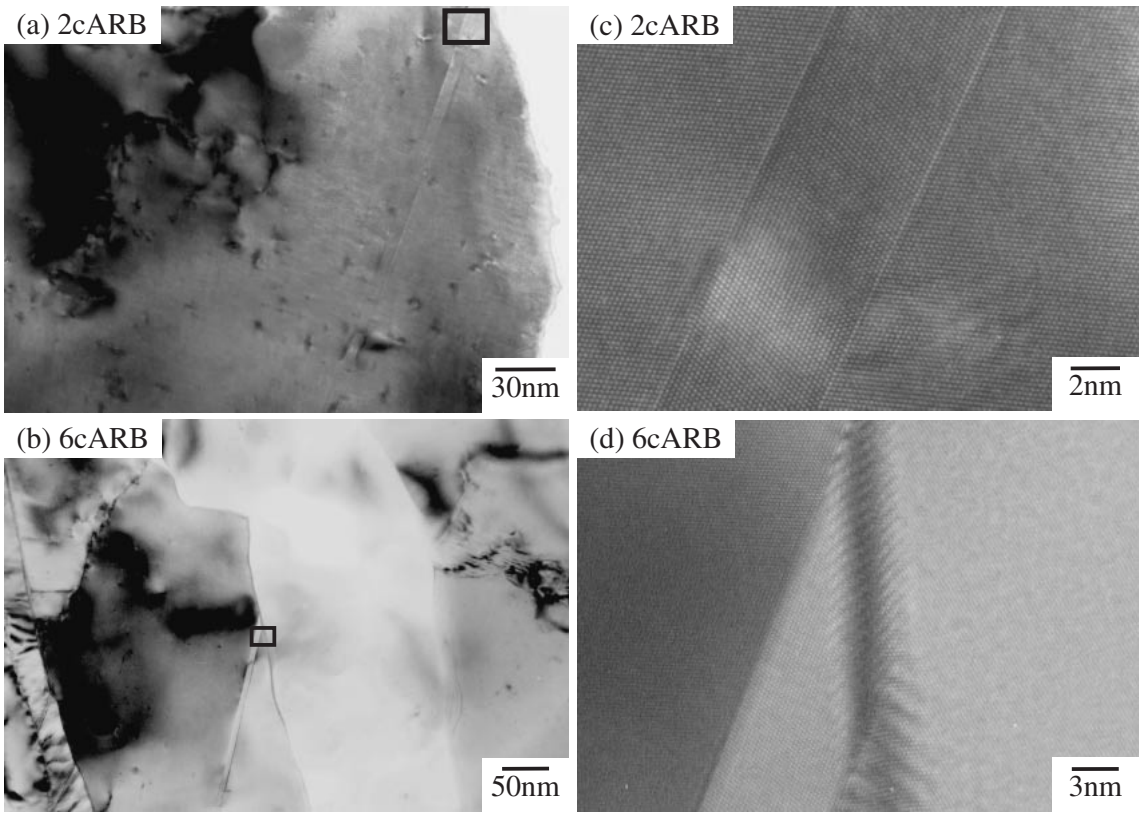


Fig. 6 TEM images of twin in (a) 2cARB-Cu and (b) 6cARB-Cu and HRTEM images of twin boundaries in (c) 2cARB-Cu and (d) 6cARB-Cu.

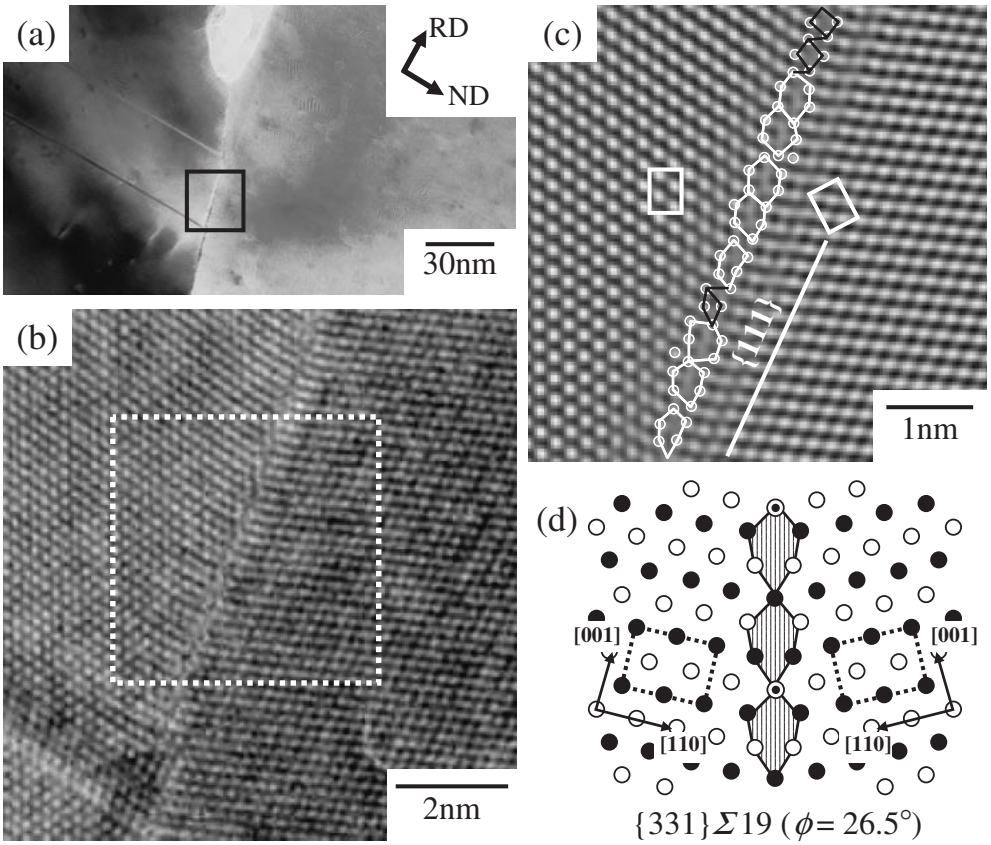


Fig. 7 (a) TEM image and (b) HRTEM image of a high angle grain boundary close to $\Sigma 19$ ATGB in 2cARB-Cu, (c) the FFT image of the dotted square region in (b) and (d) the atomic structure of the $\{331\}$ $\Sigma 19$ STGB obtained by MD simulation.

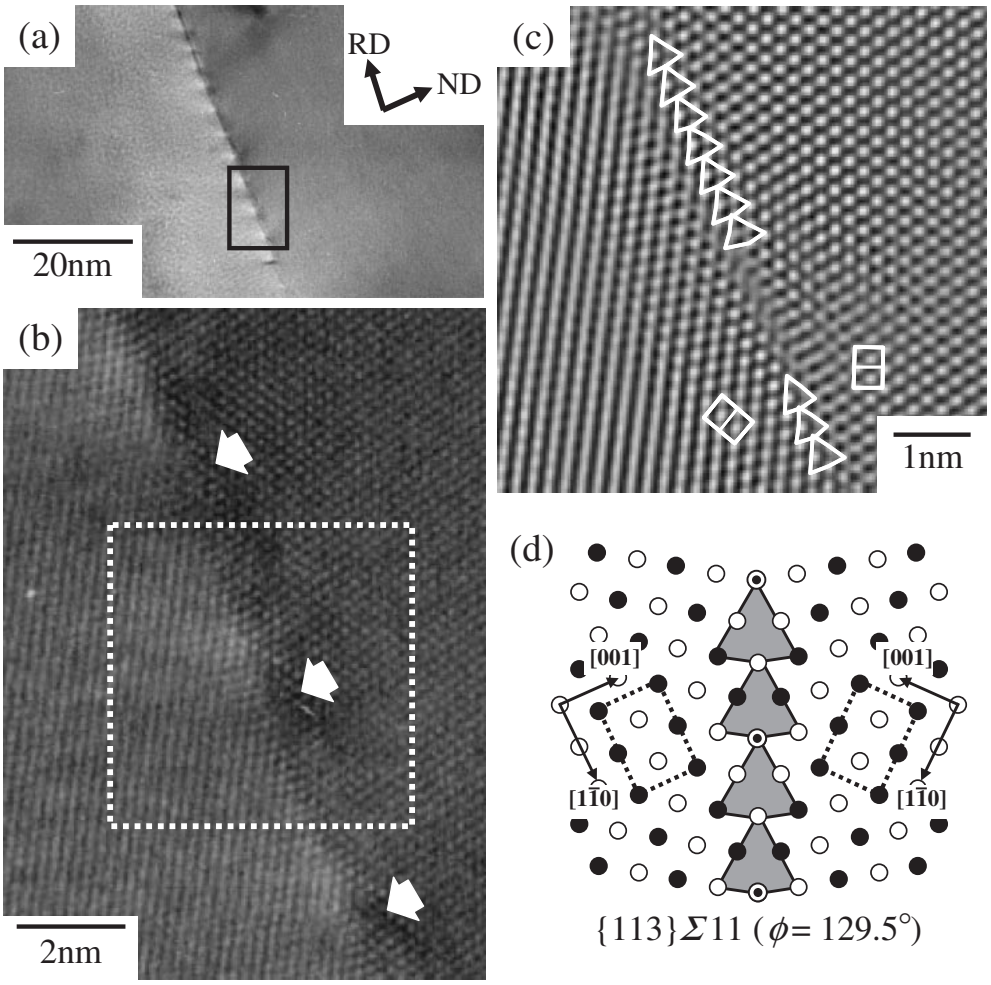


Fig. 8 (a) TEM image and (b) HRTEM image of a high angle grain boundary close to Σ11 STGB in 6cARB-Cu, (c) the FFT image of the dotted square region in (b) and (d) the atomic structure of the {113} Σ11 STGB obtained by MD simulation.

STGB planes and {110} close-packed plane, and can be also described by the structural units of these STGBs. Furthermore, in non-deformed f.c.c. metals, it was reported that the atomic structure of ATGB also consisted of the coherent planes (STGB planes etc.) and the close-packed planes.[26)]

It is generally known that the close-packed planes have very low energy in the metallic material. In case of the ATGB having different grain boundary plane from that of the STGB, the mixed structure consisting of the structural unit and the facetted coherent plane probably has lower energy than the grain boundary structure consisting of only the structural unit. Thus, it can be considered that the grain boundary faceting on the close-packed planes can occur through the atomic relaxation in vicinity of grain boundary plane of the ATGB. Therefore, these results can lead to a conclusion that the high angle boundary observed in the 2cARB-Cu in this study shows grain boundary structure similar to the most stable atomic structure of the "equilibrium" grain boundary.

Figures 8(a) and (b) show TEM and HRTEM images of high angle tilt boundary in the 6cARB-Cu, respectively. The observed grain boundary was macroscopically along RD as shown in Fig. 8(a), suggesting the observed grain boundary also corresponded to lamellar boundary within the UFG microstructure. The analysis of diffraction patterns revealed that the grain boundary had high angle misorientation of 128°, which is so close to Σ11 orientation relationship (common axis: ⟨110⟩, rotation angle: 50.5 (129.5)°). In Figs. 8(a) and (b), periodic contrasts can be pointed out on the boundary, as shown by white arrows in Fig. 8(b). These contrasts correspond with the atomic steps on the boundary which accommodate the small deviation and the twist component from the exact {113} Σ11 STGB misorientation angle. The atomic structure has been observed on a boundary not only in the SPD materials but also in the fully annealed materials.[25,27)] For comparing with the actually observed atomic structure, Figs. 8(c) and (d) show the FFT image of the dotted square region in Fig. 8(b) and the atomic structure of {113} Σ11 STGB evaluated by the MD simulation, respectively. From Figs. 8(c) and (d), it was found that the atomic structure of the region between steps can be described by single structural unit. The structural unit agrees well with that calculated for the {113} Σ11 STGB.

It can be concluded from the results shown in this section that the observed grain boundaries with large misorientations in the ARB processed Cu are basically described in terms of the structural units predicted for the normal grain boundaries. That is, the atomic structures of these grain boundaries in the ARB-Cu are similar to those of the equilibrium grain boundaries. Murayama *et al.*[28)] reported that grain interior and grain boundary structures of mechanically milled iron

had partial disclination dipoles with high strain energy by HRTEM. However, lattice defects like disclination were not observed in the present grain boundaries in the ARB-Cu.

## 4. Conclusions

In this study, an oxygen free copper was highly deformed up to strain of 4.8 by the ARB process at room temperature. The atomic structures of various grain boundaries in the ARB processed copper were observed by high resolution transmission electron microscopy and the structure was analyzed by the aid of molecular dynamics (MD) computer simulation. The main results are as follows.

(1) The MD simulation indicated that the equilibrium ⟨110⟩ symmetric tilt grain boundaries (STGB) have a misorientation angle dependence of the grain boundary energy and structure. The atomic structure of STGBs can be described by combining five kinds of structural units.

(2) The low angle boundaries in the 6cARB-Cu were basically understood in terms of conventional dislocation model. The intervals of the dislocations constructing the boundaries agreed well with those predicted from the model. In addition, however, the low angle boundaries had some distortions, like short-range curvatures of boundary plane, dense dislocations near the boundaries, and lattice bending, which would contribute to increase the boundary energy.

(3) In the 2cARB-Cu, the asymmetric tilt boundary having misorientation of 29° could be observed. The boundary plane of this grain boundary was facetted to the {111} close-packed plane and the atomic structure of this asymmetric tilt boundary could be described by structural units.

(4) In the 6cARB-Cu, a nearly symmetric tilt boundary close to the {113} $\Sigma 11$ STGB could be observed. The atomic structure of the boundary involved many steps but was described by the structural unit which is the same as that for the equilibrium ⟨110⟩ symmetric tilt boundaries calculated by MD simulation.

(5) No lattice defects with very high strain energy like disclinations was not observed in the grain boundaries observed in the present study.

(6) The present results indicate that the atomic structures of the boundaries in the Cu severely deformed by ARB are rather similar to those of the equilibrium grain boundaries, except for the local distortions which were observed in the low angle boundaries.

## Acknowledgements

The authors would like to express their hearty thanks to Prof. H. Abe for his fruitful advice and Dr. R. Ueji for his help in the experimental work. The present study was financially supported by the Grant-in-Aid for Scientific Research on Priority Area “Giant Straining Process for Advanced Materials Containing Ultra-High Density Lattice Defects” through the Ministry of Education, Culture, Sports, Science and Technology (MEXT) of Japan.

## REFERENCES

1) R. Z. Valiev, R. K. Islamgaliev and I. V. Alexandrov: Prog. Mater. Sci. **45** (2000) 103–189.
2) T. Watanabe, M. Yamada, S. Shima and S. Karashima: Philos. Mag. **A40** (1979) 667–683.
3) H. Kurishita and H. Yoshinaga: Bull. Inst. Metals **22** (1983) 944–952.
4) H. Kurishita, A. Oishi, H. Kubo and H. Yoshinaga: Trans. JIM **26** (1985) 341–352.
5) T. Tanaka, S. Tsurekawa, H. Nakashima and H. Yoshinaga: J. Japan Inst. Metals **58** (1994) 382–389.
6) K. Ikeda, K. Morita, H. Nakashima and H. Abe: J. Japan Inst. Metals **63** (1999) 179–186.
7) Z. Horita, D. J. Smith, M. Furukawa, M. Nemoto, R. Z. Valiev and T. G. Langdon: J. Mater. Res. **11** (1996) 1880–1890.
8) A. P. Sutton and V. Vitek: Philos. Trans. R. Soc. London **A309** (1983) 1–36.
9) K. Morita and H. Nakashima: Mater. Sci. Eng. **A234–236** (1997) 1053–1056.
10) J. D. Rittner and D. N. Seidman: Phys. Rev. **B54** (1996) 6999–7015.
11) G. J. Wang, A. P. Sutton and V. Vitek: Acta Metall. **32** (1984) 1093–1104.
12) H. Nakashima and M. Takeuchi: Tetsu-to-Hagane **86** (2000) 73–78.
13) Y. Saito, H. Utsunomiya, N. Tsuji and T. Sakai: Acta Mater. **47** (1999) 579–583.
14) N. Takata, K. Yamada, K. Ikeda, F. Yoshida, H. Nakashima and N. Tsuji: Mater. Trans. **48** (2007) 2043–2048.
15) N. Takata, K. Ikeda, F. Yoshida, H. Nakashima and H. Abe: J. Japan Inst. Metals **68** (2004) 240–246.
16) A. P. Sutton and J. Chen: Philos. Mag. Lett. **61** (1990) 139–146.
17) D. Wolf: Acta Metall. **38** (1990) 781–790.
18) H. Miura, X. Tong, M. Kato and T. Mori: J. Japan Inst. Metals **54** (1990) 1165–1170.
19) N. Hansen and D. J. Jensen: Philos. Trans. R. Soc. London **A357** (1999) 1447–1469.
20) X. Huang, N. Tsuji, N. Hansen and Y. Minamino: Mater. Sci. Eng. **A340** (2003) 265–271.
21) W. T. Read: *Dislocation in Crystals*, (McGraw-Hill, New York, 1953).
22) Y. H. Zhao, J. F. Bingert, X. Z. Liao, B. Z. Cui, K. Han, A. V. Sergueeva, A. K. Mukherjee, R. Z. Valiev, T. G. Langdon and Y. T. Zhu: Adv. Mater. **18** (2006) 2949–2953.
23) V. Y. Gertsman, R. Birringer, R. Z. Valiev and H. Gleiter: Scr. Metall. **30** (1994) 229–234.
24) K. Han, R. P. Walsh, A. Ishmaku, V. Toplosky, L. Brandao and J. D. Embury: Philos. Mag. **84** (2004) 3705–3716.
25) K. Ikeda, M. Kitamura, K. Morita, H. Nakashima and H. Abe: Proc. ReX ’99 (1999) 523–528.
26) K. L. Merkle: Ultramicroscopy **37** (1991) 130–152.
27) S. Tsurekawa, K. Morita, H. Nakashima and H. Yoshinaga: Mater. Trans. JIM **38** (1997) 393–400.
28) M. Murayama, J. M. Howe, H. Hidaka and S. Takaki: ISIJ Int. **43** (2003) 755–760.